IEEE Access
Multidisciplinary : Rapid Review : Open Access Journal

Received March 22, 2019, accepted April 6, 2019, date of publication April 30, 2019, date of current version May 13, 2019.

Digital Object Identifier 10.1109/ACCESS.2019.2914024

Adaptive Sliding Mode Tracking Control for Uncertain Euler-Lagrange System

ZHANKUI SONG[1] AND KAIBIAO SUN[2]
[1]School of Information Engineering, Dalian Polytechnic University, Dalian 116034, China
[2]Faculty of Electronic Information and Electrical Engineering, Dalian University of Technology, Dalian 116034, China

Corresponding author: Zhankui Song (songzhankuiwudi@163.com)

This work was supported by the Liaoning Provincial Department of Education Project under Grant 2017J044.

ABSTRACT This paper proposes an adaptive feedback control strategy–based sliding mode control technique for the EL system with actuator faults and system uncertainties. In order to obtain magnitude limited control input signal, an approximate saturation function is employed to approximate the real saturation with arbitrarily prescribed precision, and then, an auxiliary variable consists of virtual control law and adaptive control law equipped with the fuzzy logic system is introduced to compensate the adverse influence caused by uncertain nonlinear term. Specifically, on-line adaptive algorithm is derived in the sense of Lyapunov stability analysis in the closed loop design. The rigorous theoretical analysis demonstrates that the proposed control law can guarantee all the closed-loop signals, which are semi-globally uniformly ultimately bounded, and the tracking error converges to a small neighborhood of origin.

INDEX TERMS Adaptive compensation, sliding mode control, uncertain Euler-Lagrange system, fuzzy logic system.

I. INTRODUCTION

In the recent years, the tracking control problem has attracted much attention due to its applications in various nonlinear systems [1]–[5]. One of the interesting systems relevant to this problem to deal with is Euler–Lagrange (EL) systems, which encompass a wide range of non-linear mechanical systems and they are found in many practical applications. Currently, various nonlinear control strategies [6]–[9] have been proposed for EL system while numerous good results have been obtained. Nevertheless, some challenging issues still remain open. The first one is related to uncertain dynamics and external disturbances. Owing to the intrinsic nonlinearity and strong coupling, it is rather hard to obtain an accurate model for EL system that makes the model-based controllers unsuitable. On the other hand, EL systems are always under the effect of external disturbances induced by the working environmental. So, the controller design aspect for EL systems subjected to system uncertainties and external disturbances have always been a difficult task. In real word, it is important to analyze this class of nonlinear systems separately [10], [11] and to design some effective control strategy for EL systems such that the desired performance can be achieved.

The second challenging issue is about actuator faults. In practice, system actuators play a key role in generating control efforts to accomplish specific objectives. However, some unexpected faults such as the failure, loss of effectiveness or the ageing of EL systems control components are often encountered because of the harsh working environment. When actuator faults occur, the control gain matrix becomes unknown and possibly not positive definite. This problem not only degrades the control performance of EL systems, but also sometimes induces system instability. Therefore designing a tracking controller to maintain closed-loop stability and acceptable performance, despite unknown faults within the components of the EL system, is a critical issue for a real application. Many nonlinear control laws [12]–[15] have been designed using fault diagnosis and controller reconfiguration such that the adverse influence caused by actuator faults can be compensated and the stability as well as the acceptable performance of the closed-loop system can be maintained. Unfortunately, if the actuator faults are time varying and completely undetectable, the aforementioned control laws can't be applied. The robust fault tolerant control methods are a strong tool for solving the related control tasks of EL systems with time-varying and undetectable faults.

The associate editor coordinating the review of this manuscript and approving it for publication was Ning Sun.

In [16], a velocity-free fault tolerant control approach based on the sliding mode observer was proposed for EL system. In [17], a low-cost robust adaptive fault-tolerant tracking control algorithm for EL system is presented that ensures uniformly ultimately bounded stable tracking in the absence of precise target information. Chen *et al.* [18] presented a fault-tolerant cooperative control scheme for networked uncertain EL system such that the cooperative tracking of the networked system is achieved even in the presence of actuator faults and communication link faults. Hu *et al.* [19] presented the robust tracking control scheme for EL system with disturbance and multiple actuator faults, which the designed closed-loop system is also shown to be finite-time stable with the reference trajectory followed in finite time. However, the previously mentioned fault tolerant control strategies for the EL system are used in simple EL model (the parameters of generalized inertia matrix and Coriolis matrix are either completely known or partially known), few adaptive fault-tolerant control strategies for EL system with the completely unknown system parameter are reported in the literature.

In addition to the actuator faults and the adverse factors (including system uncertainties and external disturbances), actuator saturation is an important practical issue that should be considered in controller design. When an actuator entered its physical saturation limitation boundary, any operation to increase the actuator output would not make any variation of system output. Moreover, if an (actuator) unknown fault occurs, the controlled system would continue issuing its performance that may no longer be achievable by the designed controller. Under this situation, the required control output will quickly saturate the actuators while striving to maintain the "healthy" maneuvering performance. It may lead to system instability and even leading to task failure due to actuator saturation if the system is not equipped with an effective control strategy to dump the saturated actuators. Although Lyu [20], Fischer *et al.* [21], Shojaei and Chatraei [22], Zhai and Xia [23] and the references therein have developed a range of controllers to effectively handle the limited actuator output, these controllers have not considered actuator faults, and so cannot be applied directly to the FTC of EL system with limited actuator input. Although [24] provided an adaptive fault-tolerant controller for a system with actuator saturation, the controllers required large computation power and were difficult to implement.

① To deal with the effects of the saturation nonlinearity, an approximate saturation function is introduced into the controller design, which can smoothly approximate the real saturation with arbitrarily prescribed precision.

② A novel sliding surfaces with auxiliary control variable is introduced into the closed-loop system such that the adverse influence caused by uncertain nonlinear term can be suppressed.

③ Without any knowledge of system parameters and external disturbances, the continuous control input is achieved by introducing online updating laws.

II. PROBLEM FORMULATION AND PRELIMINARIES

A. SYSTEM DESCRIPTION

Consider the dynamics of nonlinear system described by Euler-Lagrange equation:

$$M(\eta)\ddot{\eta} + C(\eta,\dot{\eta})\dot{\eta} + T_d = \rho(t)\cdot sat(\tau) + \tau_b(t) \quad (1)$$

where $\eta \in \mathbb{R}^n$ represents the generalized coordinates, $\dot{\eta} \in \mathbb{R}^n$ represents the generalized velocities, $T_d \in \mathbb{R}^n$ is the lumped disturbance including the unknown gravity vector and the external disturbance, $M(\eta) \in \mathbb{R}^{n\times n}$ is the generalized inertia matrix, $C(\eta,\dot{\eta}) \in \mathbb{R}^{n\times n}$ denotes the generalized centripetal-Coriolis matrix, $M(\eta)$ and $C(\eta,\dot{\eta})$ satisfy $\|M(\eta)\| \leq \sigma_1$ and $\|C(\eta,\dot{\eta})\| \leq \sigma_2\|\dot{\eta}\|$ with positive constants σ_1 and σ_2. In this paper, the various types of actuator faults considered here are listed in Table 1, and moreover, $\rho(t) = diag\{\rho_1(t),\ldots,\rho_n(t)\} > 0$ is a continuous time-varying function reflecting the partial loss of actuator effectiveness and $\tau_b(t) \in \mathbb{R}^n$ is a function reflecting actuator bias faults.

TABLE 1. Type of actuator faults.

Types of Actuator Faults	$\rho_i(t)$	$\tau_{bi}(t)$
Healthy Actuator	1	0
Loss of Effectiveness	<1	0
Actuator Bias Fault	1	time-varying
Loss of Effectiveness with Bias Fault	<1	time-varying

In addition, $sat(\tau) = [sat(\tau_1), sat(\tau_2), \ldots, sat(\tau_n)]^T$ is the plant input subject to saturation nonlinear described by

$$sat(\tau_i) = \begin{cases} sign(\tau_i)\cdot\tau_{iM} & if \ \ |\tau_i| \geq \tau_{iM}; \\ \tau_i & if \ \ |\tau_i| < \tau_{iM}. \end{cases} \quad (2a)$$

where τ_i is the designed control input and τ_{iM} is the upper bound of $sat(\tau_i)$. From $(2a)$, the control input of EL system lies in a bounded set, i.e.,

$$\Im = \{sat(\tau_i) \mid |sat(\tau_i)| \leq \tau_{iM} < \infty\} \quad (2b)$$

In practice, the control input of EL system is likely subject to amplitude saturation with saturation bound τ_{iM}(τ_{iM} can be calculated from the physical input saturation level), therefore, $(2a)$-$(2b)$ ensure that the constraint of control input is not violated. The subsequent development is based on the assumption that η and $\dot{\eta}$ are measurable, and $M(\eta)$, $C(\eta,\dot{\eta})$, T_d, $\rho(t)$, and τ_b are unknown. It needs to be pointed out that $sat(\tau_i)$ in $(2a)$ is a non-smooth function and may not be amenable to control design for nonlinear system because the relationship between the saturation function u_i and τ_i has a sharp corner when $|\tau_i| = \tau_{iM}$. And therefore we introduce the following well-defined smooth function (3) to approximate saturation nonlinear $(2a)$ (*The saturation functions (2a) and (3) are shown in Figure 1*):

$$\Gamma(\tau_i) = \frac{1}{2c}\ln\left(\frac{e^{c\tau_{iM}}e^{c\tau_i} + e^{-c\tau_{iM}}e^{-c\tau_i}}{e^{-c\tau_{iM}}e^{c\tau_i} + e^{c\tau_{iM}}e^{-c\tau_i}}\right), \quad (3)$$

where $c > 0$ is the designed parameter and τ_{iM} is the upper bound of τ_i. Moreover, saturation nonlinear function (3) has the following Lemma1.

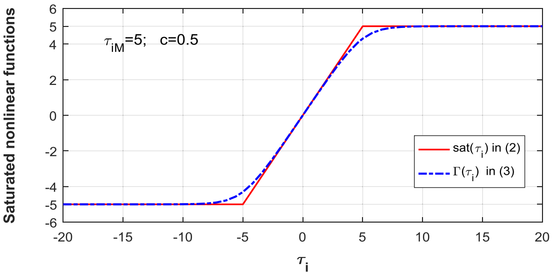

FIGURE 1. **Saturation functions $sat(\tau_i)$ and $\Gamma(\tau_i)$.**

Lemma 1: The saturation function $sat(\tau_i)$ in $(2a)$ can be expressed as

$$sat(\tau_i) = \Gamma(\tau_i) + \Delta\tau_i, \tag{4}$$

and the following properties hold.

P1: $\partial\Gamma(\tau_i)/\partial\tau_i > 0$;

P2: $\Delta\tau_i$ is bounded and $\lim\limits_{c\to+\infty} \Delta\tau_i = 0$;

P3: $|\Gamma(\tau_i)| \le \tau_{iM}$;

Proof: See the Appendix A.

Define that $x_1 = \eta$ and $x_2 = \dot{\eta}$, and combining with *Lemma1*, then system (1) can be written as

$$\begin{cases} \dot{x}_1 = x_2, \\ \dot{x}_2 = H(x_1, x_2, \dot{x}_2) + \Gamma(\tau), \end{cases} \tag{5}$$

where $H(x_1, x_2, \dot{x}_2) = (\rho(t) - 1)\cdot\Gamma(\tau) + \rho(t)\cdot\Delta\tau + \tau_b - T_d - Cx_2 - M\dot{x}_2 + \dot{x}_2$ denotes the lumped disturbance acting system.

For the development of control scheme, the following *Assumptions* and*Lemmas* are given.

Assumption 1: The state vector x_1, generalized velocity vector x_2 and acceleration vector $\dot{x}_2$ stay in a physical operation domain, denoted by $\wp$ defined as follows:

$$\wp = \{x_1,\ x_2,\ \dot{x}_2 |\ \|x_1\| \le \sigma_0,\ \|x_2\| \le \sigma_1,\ \|\dot{x}_2\| \le \sigma_2\}$$

where σ_0, σ_1, and σ_2 are unknown positive constants.

Assumption 2: The actuator effectiveness matrix $\rho(t)$ and the bias fault τ_b are continuous and satisfy $0 < \rho_i(t) \le 1$ and $\|\tau_b\| \le \sigma_3$ with a positive constant σ_3.

Assumption 3: There exists a positive constant σ_4 such that the desired command signal vector x_d satisfies $\max\{\|x_d\|, \|\dot{x}_d\|, \|\ddot{x}_d\|\} \le \sigma_4$.

*Lemma 2:*For any given scalar constant $\varsigma > 0$ and any vector $\bar{x} = [\bar{x}_1, \bar{x}_2, \ldots \bar{x}_n]^T$, the following relationship holds:

$$0 \le \|\bar{x}\| - \frac{\bar{x}^T\bar{x}}{\sqrt{\bar{x}^T\bar{x} + \varsigma^2}} < \varsigma,\ \left(\bar{x}^T\bar{x}\,\|\bar{x}\|_2^2,\ \ \|\bar{x}\|\sum\nolimits_{i=1}^{n}|\bar{x}_i|\right) \tag{6}$$

Proof: See the Appendix B.

Lemma 3 [25]. The first order sliding mode differentiator is designed as

$$\begin{cases} \dot{\eta}_{1i} = \omega_i = \eta_{2i} - b_1|\eta_{1i} - F_i(t)|^{1/2}\cdot sign(\eta_{1i} - F_i(t)), \\ \dot{\eta}_{2i} = -b_2\cdot sign(\eta_{2i} - \omega_i), \end{cases} \tag{7}$$

where η_{1i}, η_{2i}, and ω_i are the states of the system (7), b_1 and b_2 are positive design constants, and $F_i(t)$ is a known function. Then, ω_i can approximate the differential term $\dot{F}_i(t)$ to any arbitrary accuracy if the initial deviations $\eta_{1i} - F_i(t_0)$ and $\omega_i - \dot{F}_i(t_0)$are bounded.

Remark 1: In application, the information acquisition of some states is achieved through physical sensors. However, the detection output of a healthy physical sensor has the maximum operation range. That means system sates stay in a physical operation domain. Therefore, Assumption 1 ensures that EL system sates do not extend to infinity, which is true in all physical plant.

B. DESCRIPTION OF A FUZZY LOGIC SYSTEM

A fuzzy logic system can approximate any continuous functions on a compact set to an arbitrary accuracy [26]. It is composed of four principal components: an inference engine, a fuzzy rule, a fuzzifier, and a defuzzifier. The fuzzy logic system can be formed by a set of 'If-Then' linguistic rules, i.e.,

$$R^{(j)}:\ If\ x_1 is\ A_1^j\ and\ \ldots\ and\ x_n\ is\ A_n^j,\ Then\ z\ is\ B^j$$

where $j = 1, 2, \ldots, N$, $x = (x_1, x_2, \ldots, x_n)^T$ and $z \in \mathbb{R}$ are the inputs and output of the fuzzy logic system, respectively. In addition, A_i^j, $i = 1, 2, \ldots, N$, and B_i^j are characterized by fuzzy membership function $\mu_{A_i^j}(x_i)$ and $\mu_{B_i^j}(z)$, respectively. Based on singleton fuzzifier, product inference, center-average defuzzifier, and Gaussian membership function, output of the Fuzzy logic system can be written as

$$f(x) = \sum\nolimits_{j=1}^{M} \frac{\bar{z}^j\left(\prod_{i=1}^{n}\mu_{A_i^j}(x_i)\right)}{\sum_{j=1}^{M}\left(\prod_{i=1}^{n}\mu_{A_i^j}(x_i)\right)} = \boldsymbol{\Phi}\cdot\boldsymbol{\zeta}(x), \tag{8}$$

where $\bar{z}^j \in \mathbb{R}$ is the point at which $\mu_{B_i^j}(z)$ achieves the maximum value, $\boldsymbol{\Phi} = \left[\bar{z}^1, \bar{z}^2, \ldots, \bar{z}^M\right]$ is an adjustable parameter vector. And $\boldsymbol{\zeta} = [\zeta_1(x), \zeta_2(x), \ldots, \zeta_n(x)]$ is the fuzzy basis function vector, each element of $\boldsymbol{\zeta}(x)$ is

$$\zeta_i(x) = \sum\nolimits_{j=1}^{M} \frac{\prod_{i=1}^{n}\mu_{A_i^j}(x_i)}{\sum_{j=1}^{M}\left(\prod_{i=1}^{n}\mu_{A_i^j}(x_i)\right)}. \tag{9}$$

It should be pointed out that the fuzzy logic system are able to approximate a continuous function defined on a compact set to any given accuracy, which can effectively deal with uncertainty [27]. For a continuous nonlinear function H, which can be approximated by

$$H(x_1, x_2, \dot{x}_2) = f(x) = \boldsymbol{\Phi}\cdot\boldsymbol{\zeta}(x) + \boldsymbol{\varepsilon}, \tag{10}$$

where $\boldsymbol{\Phi} = [\Phi_1, \Phi_2, \ldots, \Phi_n]^T$ is an optimal weight vector and $\boldsymbol{\varepsilon} = [\varepsilon_1, \varepsilon_2, \ldots, \varepsilon_n]^T$ is the approximation error.

Assumption 4: The optimal weight and approximation error of FLS are bounded such that

$$\|\boldsymbol{\Phi}\| \le \lambda \text{ and } \|\boldsymbol{\varepsilon}\| \le \varepsilon_M, \tag{11}$$

where λ and ε_M are positive constants.

C. PROBLEM FORMULATION

The main problem to be investigated in this study can be formulated as: For the systems described by (5), design a closed-loop system to achieve the objective of tracking control. More specifically, given any bounded desired command x_d, develop a control input τ_i to guarantee that x_d can be followed even in the presence of actuator faults and uncertainties.

III. MAIN RESULTS

In this subsection, a closed-loop control structure will be proposed for EL system, and the control algorithm can guarantee that the closed-loop tracking system is UUB stable. To achieve high-accuracy tracking control, a virtual compensation version of the proposed control method is further designed to handle the lumped disturbance in the system. To fully show the compensation control design, the tracking error and its dynamics are defined as follows.

$$e_1 = [e_{11}, e_{12}, \ldots, e_{1n}]^T = x_1 - x_d, \tag{12}$$

$$e_2 = \dot{e}_1 = \dot{x}_1 - \dot{x}_d = x_2 - \dot{x}_d. \tag{13}$$

Then a dynamic sliding surface S_a and an auxiliary variable z are defined as

$$S_a = [S_{a1}, S_{a2}, \ldots, S_{a3}]^T = e_2 + c_1 \cdot e_1 + c_2 \cdot z, \tag{14}$$

$$z = [z_1, z_2, \ldots, z_n]^T = \Gamma(\tau) - \boldsymbol{\varphi} - \Xi, \tag{15}$$

where $z(0) = 0$, $\boldsymbol{\varphi}[\varphi_1, \ldots, \varphi_n]^T$ and $\Xi[\Xi_1, \ldots, \Xi_n]^T$ are regarded as virtual control law and auxiliary control law, respectively, which $\boldsymbol{\varphi}$ and Ξ will be designed later. It is worth mentioning that the design parameters c_1 and c_2 need to satisfy $c_1 > 0$ and $c_2 < -1$. From (5), (10), and (15), the derivative of S_a is given as follows

$$\begin{aligned}\dot{S}_a &= \left[\dot{S}_{a1}, \dot{S}_{a2}, \ldots, \dot{S}_{ai}\right]^T = \dot{x}_2 - \ddot{x}_{1d} + c_1 \cdot \dot{e}_1 + c_2 \cdot \dot{z}\\ &= H(x_1, x_2, \dot{x}_2) + \Gamma(\tau) - \ddot{x}_{1d} + c_1 \cdot \dot{e}_1 + c_2 \cdot \dot{z}.\\ &= \boldsymbol{\Phi} \cdot \boldsymbol{\zeta}(x) + \boldsymbol{\varepsilon} + z + \boldsymbol{\varphi} + \Xi - \ddot{x}_{1d} + c_1 \cdot \dot{e}_1 + c_2 \cdot \dot{z}.\end{aligned} \tag{16}$$

Considering (14), multiplying both sides of the resultant equality by S_a and noting (13), one obtains

$$\begin{aligned}S_a^T \dot{S}_a = {} & S_a^T \cdot \boldsymbol{\Phi} \cdot \boldsymbol{\zeta}(x) + S_a^T \boldsymbol{\varepsilon} + S_a^T (z + \boldsymbol{\varphi} + \Xi - \ddot{x}_{1d})\\ & + S_a^T c_1 \dot{e}_1 + S_a^T c_2 \cdot \left(\left(\partial\Gamma(\tau)/\partial\tau\right) \cdot \dot{\tau} - \dot{\boldsymbol{\varphi}} - \dot{\Xi}\right).\end{aligned} \tag{17}$$

By using young's inequality with $\delta \in \mathbb{R}^+$, we have

$$\begin{cases} S_a^T \boldsymbol{\varepsilon} \le \|S_a\|_2^2/2\delta^2 + \delta^2 \|\boldsymbol{\varepsilon}\|_2^2/2,\\ S_a^T \cdot \boldsymbol{\Phi} \cdot \boldsymbol{\zeta}(x) \le \|S_a\| \cdot \lambda \cdot \|\boldsymbol{\zeta}\|. \end{cases} \tag{18}$$

Applying (18), then (17) can be rewritten as

$$\begin{aligned}S_a^T \dot{S}_a \le {} & \|S_a\| \cdot \lambda \cdot \|\boldsymbol{\zeta}\| + \|S_a\|_2^2 \Big/ 2\delta^2 + \delta^2 \|\boldsymbol{\varepsilon}\|_2^2 \Big/ 2\\ & + S_a^T \cdot z + S_a^T \cdot (\boldsymbol{\varphi} + \Xi) + S_a^T \cdot \kappa_1\\ & + S_a^T c_2 \cdot \left(\left(\partial\Gamma(\tau)/\partial\tau\right) \cdot \dot{\tau} - \dot{\boldsymbol{\varphi}} - \dot{\Xi}\right)\\ & \underbrace{- \kappa_2 \|S_a\|_2^2 + \kappa_2 \|S_a\|_2^2 - \left|S_a^T \kappa_1\right| + \left|S_a^T \kappa_1\right|}_{is\ zero},\end{aligned} \tag{19}$$

where $\kappa_1[\kappa_{11}, \kappa_{12}, \ldots \kappa_{1n}]^T = c_1 \cdot \dot{e}_1 - \ddot{x}_{1d}$ and $\kappa_2 = \eta_1 + 1$.

Design the virtual control law $\boldsymbol{\varphi}$ and auxiliary control law Ξ as follows

$$\boldsymbol{\varphi} = -\frac{\kappa_2^2 \cdot \|S_a\|_2^2 \cdot S_a}{\sqrt{\kappa_2^2 \cdot \|S_a\|_2^4 + \varsigma^2}} - \frac{\|\kappa_1\|_2^2 \cdot S_a}{\sqrt{\|\kappa_1\|_2^2 \cdot \|S_a\|_2^2 + \varsigma^2}}, \tag{20}$$

$$\Xi = -\frac{\hat{\lambda}^2 \cdot \|\boldsymbol{\zeta}\|_2^2 \cdot S_a}{\sqrt{\hat{\lambda}^2 \cdot \|\boldsymbol{\zeta}\|_2^2 \cdot \|S_a\|_2^2 + \varsigma^2(t)}}, \tag{21}$$

here, adaptive parameter $\hat{\lambda}$ can be updated as follows

$$\dot{\hat{\lambda}} = \gamma \cdot \left(\|S_a\| \cdot \|\boldsymbol{\zeta}\| - a \cdot \hat{\lambda}\right), \hat{\lambda}(0) > 0, \tag{22}$$

where $\gamma \in \mathbb{R}^+$ and $a \in \mathbb{R}^+$ are the design parameters.

Remark 2: The virtual control law $\boldsymbol{\varphi}$ and auxiliary variable Ξ are employed in cooperative compensation control strategy design. The virtual control law $\boldsymbol{\varphi}$ consists of the linear feedback term and control gain adjustment term for control accuracy of the closed-loop system. Auxiliary variable Ξ is the compensation term for the lumped disturbance including system uncertainties, actuation faults and external disturbances.

It is worth noting the time derivative of Ξ and $\boldsymbol{\varphi}$ are required for the subsequent stability analysis and control law design. However, taking the time derivative of the auxiliary variable Ξ may cause the explosion problem of a complex term. To eliminate this problem, the following first order sliding mode differentiator according to Lemma 3 is adopted to estimate each element of $\dot{\Xi}$ and $\dot{\boldsymbol{\varphi}}$:

$$\begin{cases} \dot{\eta}_{1i} = \omega_i = \eta_{2i} - b_1 \left|\eta_{1i} - \Xi_i - \varphi_i\right|^{1/2} \cdot sign\left(\eta_{1i} - \Xi_i - \varphi_i\right),\\ \dot{\eta}_{2i} = -b_2 \cdot sign\left(\eta_{2i} - \omega_i\right), \end{cases} \tag{23}$$

where η_{1i}, η_{2i}, and ω_i are the states of the system (18), and b_1 and b_2 are design parameters. Based on (23) and Lemma 3, we obtain

$$\dot{\Xi} + \dot{\boldsymbol{\varphi}} = \boldsymbol{\omega} + \boldsymbol{\chi}, \tag{24}$$

where $\boldsymbol{\omega} = [\omega_1, \omega_2, \ldots, \omega_n]^T$, and $\boldsymbol{\chi} = [\chi_1, \chi_2, \ldots, \chi_n]^T$ is the estimation error vector of the first order sliding mode differentiator. In the light of Lemma 3, we have $\|\boldsymbol{\chi}\|^2 \le \beta$ with a small positive constant β.

To proceed, we define $\tilde{\lambda} = \lambda - \hat{\lambda}$. From (19), (20), (21) (22), and (24), we further obtain that

$$\begin{aligned}& S_a^T \dot{S}_a - \gamma^{-1} \cdot \tilde{\lambda}\dot{\hat{\lambda}}\\ & \le \|S_a\| \cdot \lambda \cdot \|\boldsymbol{\zeta}\| - \|S_a\| \cdot \tilde{\lambda} \cdot \|\boldsymbol{\zeta}\| + a \cdot \tilde{\lambda} \cdot \hat{\lambda} + \|S_a\|_2^2 \Big/ 2\delta^2\\ & \quad + \delta^2 \|\boldsymbol{\varepsilon}\|_2^2 \Big/ 2 - \eta_1 \cdot \|S_a\|_2^2 - \|S_a\|_2^2 + \kappa_2 \|S_a\|_2^2 + \left|S_a^T \kappa_1\right|\\ & \quad - \frac{\kappa_2^2 \cdot \|S_a\|_2^4}{\sqrt{\kappa_2^2 \cdot \|S_a\|_2^4 + \varsigma^2}} - \frac{\|\kappa_1\|_2^2 \cdot \|S_a\|_2^2}{\sqrt{\|\kappa_1\|_2^2 \cdot \|S_a\|_2^2 + \varsigma^2}} + S_a^T \cdot z\end{aligned}$$

$$- \frac{\hat{\lambda}^2 \cdot \|\boldsymbol{\zeta}\|_2^2 \cdot \|S_a\|_2^2}{\sqrt{\hat{\lambda}^2 \cdot \|\boldsymbol{\zeta}\|_2^2 \cdot \|S_a\|_2^2 + \varsigma^2}} + S_a^T c_2 \left(\frac{\partial \Gamma(\tau)}{\partial \tau} \cdot \dot{\tau} - \boldsymbol{\omega} - \boldsymbol{\chi} \right). \quad (25)$$

In light of Lemma 2 and the definition $S_a = e_2 + c_1 e_1 + c_2 z$, one can find that

$$\begin{cases} (1) - \dfrac{\kappa_2^2 \|S_a\|_2^4}{\sqrt{\kappa_2^2 \cdot \|S_a\|_2^4 + \varsigma^2}} + \kappa_2 \|S_a\|_2^2 \le \varsigma, \\ (2) - \dfrac{\|\kappa_1\|_2^2 \cdot \|S_a\|_2^2}{\sqrt{\|\kappa_1\|_2^2 \cdot \|S_a\|_2^2 + \varsigma^2}} + \left|S_a^T \kappa_1\right| \le \varsigma, \\ (3) - \dfrac{\hat{\lambda}^2 \cdot \|\boldsymbol{\zeta}\|_2^2 \cdot \|S_a\|_2^2}{\sqrt{\hat{\lambda}^2 \cdot \|\boldsymbol{\zeta}\|_2^2 \cdot \|S_a\|_2^2 + \varsigma^2}} + \|S_a\| \cdot \left|\hat{\lambda}\right| \cdot \|\boldsymbol{\zeta}\| \le \varsigma, \\ (4) - S_a^T S_a = -\|S_a\|_2^2 \\ = -\|e_2 + e_1\|^2 - c_2^2 \|z\|^2 - 2c_2 [e_2 + e_1]^T z \\ \le -\|e_2 + e_1\|^2 - c_2^2 \|z\|^2 + c_2 \left(\|z\|^2 + \|e_2 + e_1\|^2\right) \\ = -(1 - c_2) \cdot \|e_2 + e_1\|^2 - \left(c_2^2 - c_2\right) \cdot \|z\|^2. \end{cases} \quad (26)$$

From (26), one has

$$\begin{aligned} & S_a^T \dot{S}_a - \gamma^{-1} \cdot \tilde{\lambda}\dot{\hat{\lambda}} \\ & \le -\left(\eta_1 - \frac{1}{2\delta^2}\right) \cdot \|S_a\|_2^2 + a\tilde{\lambda}\hat{\lambda} + \frac{\delta^2 \|\boldsymbol{\varepsilon}\|_2^2}{2} \\ & \quad - (1 - c_2) \cdot \|e_2 + c_1 \cdot e_1\|^2 - \left(c_2^2 - c_2\right) \cdot \|z\|^2 \\ & \quad + 3 \cdot \varsigma + S_a^T z + S_a^T c_2 \left(\frac{\partial \Gamma(\tau)}{\partial \tau} \cdot \dot{\tau} - \boldsymbol{\omega} - \boldsymbol{\chi} \right). \end{aligned} \quad (27)$$

Now we are ready to provide the following the input updating law:

$$\dot{\tau} = \left(\frac{\partial \Gamma(\tau)}{\partial \tau} \right)^{-1} \cdot \left(\boldsymbol{\omega} - \frac{z}{c_2} \right), \quad (\tau(0) = 0) \quad (28)$$

where $(\partial\Gamma(\tau)/\partial\tau)^{-1}$ $diag\left\{(\partial\Gamma(\tau_1)/\partial\tau_1)^{-1}, \ldots, (\partial\Gamma(\tau_n)/\partial\tau_n)^{-1}\right\}$.

The following theorem established the criteria for choosing the controller parameters to warrant the stability of the tracking error e_1.

Theorem 1: Consider the dynamics system described by (5). Suppose that Assumptions 1-3 hold. Under the designed closed-loop system consisted by (20), (21), (22), and (28), if the controller parameters c_1, c_2, and η_1 satisfy

$$\begin{cases} 2\eta_1 - \delta^{-2} - c_2^2 > 0, & c_1 > 0, \\ c_2^2 - 2c_2 - 2 > 0, & c_2 < -1, \end{cases} \quad (29)$$

then the following conclusions hold:

1) all closed-loop signals are bounded;

2) the tracking errors e_{1i} and auxiliary variables z_i $(i = 1, 2, \ldots, n)$ will converge into a bounded set.

Proof: Consider the Lyapunov candidate function as

$$V(t) = \frac{1}{2} S_a^T S_a + \frac{1}{2} |c_2| \cdot z^T z + \frac{1}{2\gamma} \tilde{\lambda}^2. \quad (30)$$

Taking the time derivative of $V(t)$ and using (27)-(28), we have

$$\begin{aligned} \dot{V}(t) & \le -\left(\eta_1 - \frac{1}{2\delta^2}\right) \cdot \|S_a\|_2^2 + a\tilde{\lambda}\hat{\lambda} \\ & \quad + \frac{\delta^2 \|\boldsymbol{\varepsilon}\|_2^2}{2} - \left(c_2^2 - c_2\right) \cdot \|z\|^2 \\ & \quad - (1 - c_2) \cdot \|e_2 + c_1 e_1\|^2 + S_a^T c_2 \left(\frac{\partial \Gamma(\tau)}{\partial \tau} \cdot \dot{\tau} - \boldsymbol{\omega} - \boldsymbol{\chi} \right) \\ & \quad + 3 \cdot \varsigma(t) + S_a^T \cdot z + |c_2| \cdot z^T \cdot \left(\frac{\partial \Gamma(\tau)}{\partial \tau} \cdot \dot{\tau} - \boldsymbol{\omega} - \boldsymbol{\chi} \right) \\ & = -\left(\eta_1 - \frac{1}{2\delta^2}\right) \cdot \|S_a\|_2^2 + a\tilde{\lambda}\hat{\lambda} + \frac{\delta^2 \|\boldsymbol{\varepsilon}\|_2^2}{2} \\ & \quad - \left(c_2^2 - c_2\right) \cdot \|z\|^2 \\ & \quad - (1 - c_2) \cdot \|e_2 + c_1 e_1\|^2 + 3 \cdot \varsigma \\ & \quad - S_a^T c_2 \boldsymbol{\chi} + z^T z + z^T c_2 \boldsymbol{\chi}. \end{aligned} \quad (31)$$

Again, using the young's inequality

$$\begin{cases} a\tilde{\lambda}\hat{\lambda} \le -a\gamma\tilde{\lambda}^2 / 2\gamma + a\lambda^2/2 \\ z^T c_2 \boldsymbol{\chi} \le c_2^2 \|z\|_2^2/2 + \|\boldsymbol{\chi}\|_2^2/2 \\ S_a^T c_2 \boldsymbol{\chi} \le c_2^2 \|S_a\|_2^2/2 + \|\boldsymbol{\chi}\|_2^2/2 \end{cases} \quad (32)$$

Then, we further get that

$$\begin{aligned} \dot{V}(t) & \le -\left(\eta - \frac{1}{2\delta^2} - \frac{c_2^2}{2}\right) \cdot \|S_a\|_2^2 \\ & \quad - \left(\frac{c_2^2}{2} - c_2 - 1\right) \cdot \|z\|^2 - \frac{a\gamma\tilde{\lambda}^2}{2\gamma} + \Delta_g \\ & \le -\varpi \cdot V(t) + \Delta_g \end{aligned} \quad (33)$$

where $\varpi = \min\left\{\left(2\eta - \delta^{-2} - c_2^2\right), \ \left(c_2^2 - 2c_2 - 2\right), \ a\gamma\right\}$ and $\Delta_g = 0.5 \cdot \left(a \cdot \lambda^2 + \delta^2 \cdot \|\boldsymbol{\varepsilon}\|_2^2\right) + 3 \cdot \varsigma + \beta$.

Integrating both sides of (33), it is obtained that

$$V(t) \le \frac{\Delta_g}{\varpi} + \left(V(0) - \frac{\Delta_g}{\varpi}\right) e^{-\varpi t} < +\infty, \quad (34)$$

Combining (30) and (34), we further obtain that $\lim_{t\to\infty} |S_{ai}| \le \sqrt{2\Delta_g/\varpi}$ and $\lim_{t\to\infty} |z_i| \le \sqrt{2\Delta_g/\varpi \cdot |c_2|}$. From (14), we obtain $\lim_{t\to\infty} |\dot{e}_{1i} + c_1 \cdot e_{1i}| \le 2 \cdot \sqrt{2\Delta_g/\varpi}$.

To facilitate the further analysis of tracking error, we denote

$$\upsilon_i(t) = \dot{e}_{1i} + c_1 \cdot e_{1i} \quad (35)$$

Solving the first differentiate equation in (35) yields

$$e_{1i}(t) = e^{-c_1 \cdot t} \cdot e_{1i}(0) + e^{-c_1 \cdot t} \cdot \int_0^t \upsilon_i(\vartheta) \cdot e^{c_1 \cdot \vartheta} d\vartheta. \quad (36)$$

From (36), we can see that if $\int_0^t \upsilon_i(\vartheta) \cdot e^{c_1 \cdot \vartheta} d\vartheta$ is bounded, then $e_{1i}(t) \to 0$ as $t \to \infty$. If, however, $\int_0^t \upsilon_i(\vartheta) \cdot e^{c_1 \cdot \vartheta} d\vartheta$ is unbounded, we then use the L' Hopital's rule to (36) and obtain

$$\lim_{t\to\infty} e_{1i}(t) = 0 + \lim_{t\to\infty} \frac{\upsilon_i(t) \cdot e^{c_1 \cdot t}}{c_1 \cdot e^{c_1 \cdot t}} = \lim_{t\to\infty} \frac{\upsilon_i(t)}{c_1} \quad (37)$$

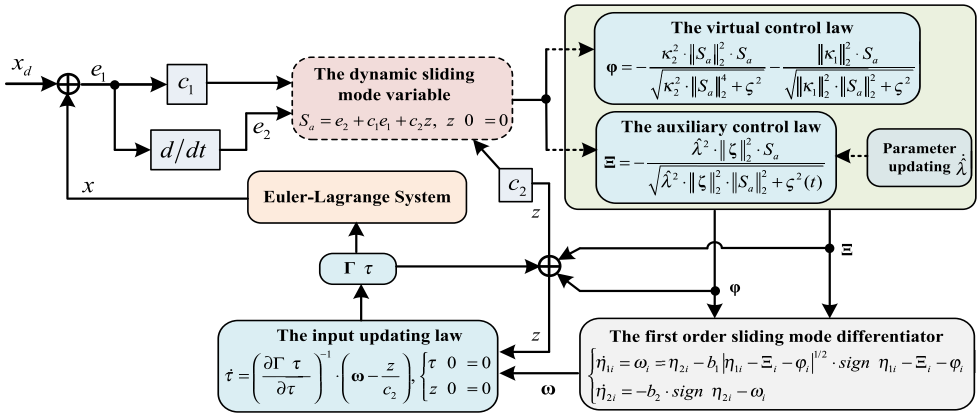

FIGURE 2. The closed-loop system structure.

which implies that if $\upsilon_i(t)$ is bound as $t \to \infty$, then $\lim_{t\to\infty} |e_{1i}| \le 2 \cdot \sqrt{2\Delta_g/\varpi}\Big/c_1$. Based on the above analysis, it is easy to conclude that z_i, e_{1i} and $\dot{e}_{1i}$ are ultimately confined in the following compact set, respectively:

$$\Omega_z = \left\{ z_i \mid \ |z_i| \le \sqrt{2\Delta_g/\varpi \cdot |c_2|} \right\} \tag{38}$$

$$\Omega_e = \left\{ e_{1i} \mid \ |e_{1i}| \le 2 \cdot \sqrt{2\Delta_g/\varpi}\Big/c_1 \right\} \tag{39}$$

$$\Omega_{\dot{e}} = \left\{ \dot{e}_{1i} \mid \ |\dot{e}_{1i}| \le 2 \cdot \sqrt{2\Delta_g/\varpi} \right\} \tag{40}$$

Thus, we complete the whole proof. □

To facilitate the readers to understand the control strategy, the overall architecture of the designed method is given in Fig. 2.

Remark 3: In light of (34), we see that the parameters of close-loop systems c_1, c_2, δ, a, andγ determine the size of the tracking errors, that is, the smaller the tracking errors, the bigger the control parameters c_1, $|c_2|$, and η should be. Since the design parameters δ and a can be set as small as possible, hence Δ_g in (33) can be adjusted to a small boundary, i.e., the tracking errors are guaranteed to be small enough by choosing the small parameters δ, ς and a.

IV. NUMERICAL SIMULATIONS

In this section, the developed control method is applied to an uncertain two-link robotic manipulator system in the presence of the actuation faults and adverse factors to demonstrate the effectiveness. The developed method is applied on a two-link robotic manipulator given by

$$M(\eta)\ddot{\eta} + C(\eta,\dot{\eta})\dot{\eta} + T_d = \rho(t) \cdot sat(\tau) + \tau_b$$

where $\eta = \begin{bmatrix} \eta_1 \\ \eta_2 \end{bmatrix}$, $M = \begin{bmatrix} M_{11} & M_{12} \\ M_{21} & M_{22} \end{bmatrix}$, $C = \begin{bmatrix} C_{11} & C_{12} \\ C_{21} & 0 \end{bmatrix}$, $T_d = \begin{bmatrix} T_{d1} \\ T_{d2} \end{bmatrix}$, $\tau_b = \begin{bmatrix} \tau_{b1} \\ \tau_{b2} \end{bmatrix}$, and $\rho = \begin{bmatrix} \rho_1 & 0 \\ 0 & \rho_2 \end{bmatrix}$. Here, η_1 and η_2 represent the joint angles of the first and second links, respectively. $M_{11} = (m_1 + m_2) \cdot r_1^2 + m_2 \cdot r_2^2 + 2m_2 r_1^2 r_2^2 \cdot \cos(\eta_2)$, $M_{12} = M_{21} = m_2 r_2^2 + m_2 r_1 r_2 \cos(\eta_2)$, $M_{22} = m_2 r_2^2$,$C_{11} = -p\dot{\eta}_2 \sin(\eta_2)$, $C_{21} = p\dot{\eta}_1 \sin(\eta_2)$ with $p = 0.242kgm^2$. In addition, the parameters of manipulators are set as follows. The masses of links 1 and 2 are $m_1 = m_2 = 2kg$. The link lengths are $r_1 = r_2 = 1\,m$. Let initial conditions of system states be $\eta(0) = [0.05,\ 0.1]^T$ and $\dot{\eta}(0) = [0,\ 0]^T$. The parameters of closed-loop system are chosen as $c_1 = 2$, $c_2 = -2$, $\delta = \varsigma = 0.5$, $\eta_1 = \gamma = 6$, $\tau_{iM} = 30$, and $a = 0.1$. In (23), the parameters of first order sliding mode differentiator are selected as $b_1 = b_2 = 15$. To implement the adaptive fuzzy system, the membership function are given as

$$\mu_{A_i^1}(x_i) = \exp[-((x_i + \pi/6)/(\pi/24))^2],$$

$$\mu_{A_i^2}(x_i) = \exp\left[-((x_i + \pi/12)/(\pi/24))^2\right],$$

$$\mu_{A_i^3}(x_i) = \exp\left[-(x_i/(\pi/24))^2\right],$$

$$\mu_{A_i^4}(x_i) = \exp\left[-((x_i - \pi/12)/(\pi/24))^2\right],$$

$$\mu_{A_i^5}(x_i) = \exp[-((x_i - \pi/6)/(\pi/24))^2].$$

In simulation, the control objective is to track the desired trajectory $\eta_d = [\eta_{1d},\ \eta_{2d}]^T = x_d = [0.3\sin t,\ \ 0.2\cos t]^T$.

To show the effectiveness of the proposed control strategy, simulation results are obtained for two cases included the actuator fault and the others adverse factors, while maintaining the remaining conditions unchanged.

Case 1: $T_{d1} = T_{d2} = 15 \cdot \dot{\eta}_1 + 6 \cdot \mathrm{sign}(\dot{\eta}_1)$, $\rho_1 = 0.75$, $\rho_2 = 0.8$, and $\tau_{b1} = \tau_{b2} = 0.2 \cdot \sin(2t)$.

The results are presented in Fig. 3, which shows that the system states are indeed bounded, which clearly indicates that z_i, e_{1i}, $\dot{e}_{1i}$, and S_{ai} $(i = 1, 2)$ are all retained, as claimed in Theorem 1. Moreover, we can also observe that $\eta_1 - \eta_{1d}$ and $\eta_2 - \eta_{2d}$ converge to a small neighborhood of stable point $(|\eta_1 - \eta_{1d}| \le 1.8 \times 10^{-3} rad$, $|\eta_2 - \eta_{2d}| \le 5 \times 10^{-4} rad\ for\ t \ge 1s)$ which indicates that the proposed control strategy is effective to suppress the adverse factors including disturbance, system uncertainty, and actuator fault. From Figs. 4-5, it can be seen that the initial amplitude value

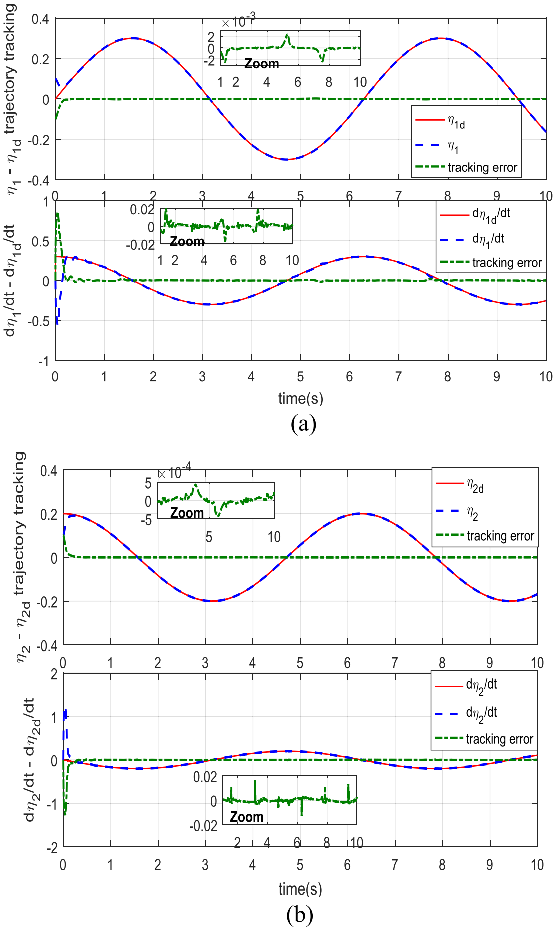

FIGURE 3. (a)-(b). System states trajectory tracking under case 1. (a) $\eta_1-\eta_{1d}$ and $\dot\eta_1-\dot\eta_{1d}$ tracking. (b) $\eta_2-\eta_{2d}$ and $\dot\eta_2-\dot\eta_{2d}$ tracking.

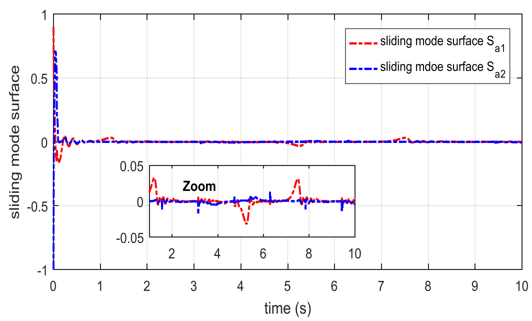

FIGURE 4. Sliding mode variables under case 1.

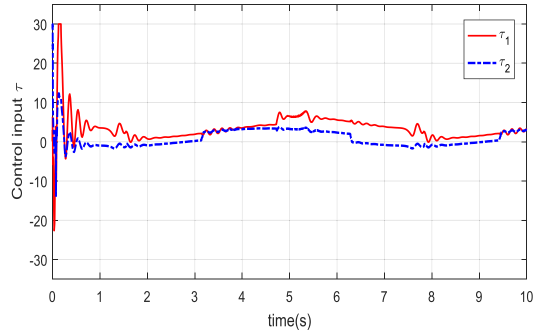

FIGURE 5. Control input τ under case 1.

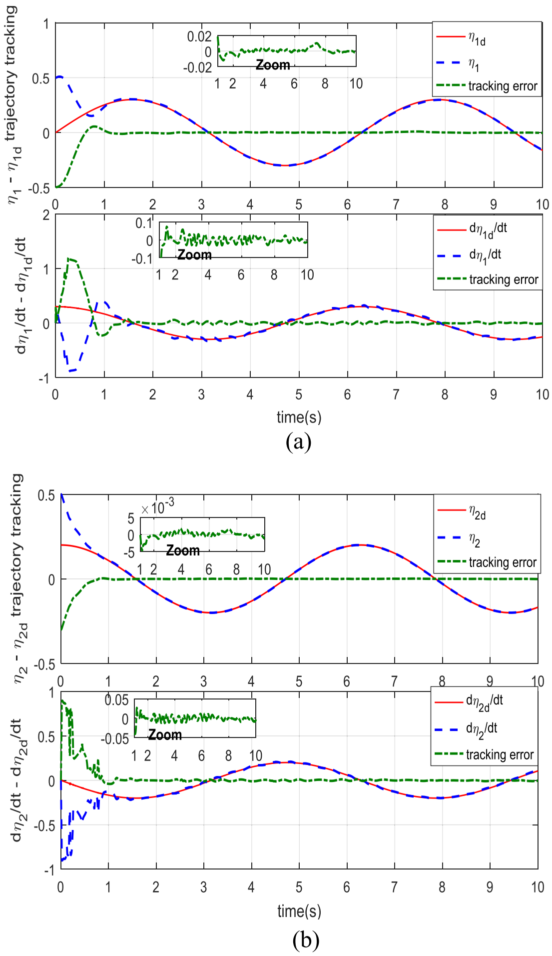

FIGURE 6. (a)-(b). System states trajectory tracking under case 2. (a) $\eta_1-\eta_{1d}$ and $\dot\eta_1-\dot\eta_{1d}$ tracking. (b) $\eta_2-\eta_{2d}$ and $\dot\eta_2-\dot\eta_{2d}$ tracking.

of input updating value τ_i and sliding surface variable S_{ai} are large, This is because that the proposed method is tuning and do not adapt to the adverse factors at the beginning. And then the adaptation updating algorithm starts to exert its effectiveness such that the satisfactory control performance is achieved.

Case 2: $T_{d1} = T_{d2} = 20\dot\eta_1 + 10\text{sign}(\dot\eta_1)$, $\rho_1 = 0.55 + 0.15\sin(t)$, $\rho_2 = 0.65 + 0.15 \cdot \sin(t)$, and $\tau_{b1} = \tau_{b2} = 0.8 \cdot \sin(2t)$.

From Figs. 6–8 by using the proposed method, the system state trajectories achieve its maximum at the beginning of the engagement, and stays at a stable boundary at the rest. Compared with Case 1, although uncertainties and disturbance are increased under actuator fault, the high tracking accuracy and fast convergence are still hold, and namely the adverse factors are well suppressed. These simulation results show that the good performance can be obtained under the proposed control algorithm.

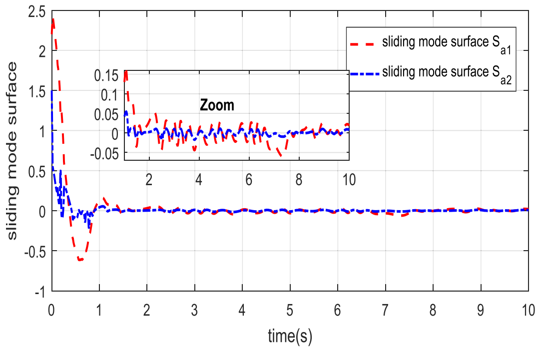

FIGURE 7. Sliding mode variables under case 2.

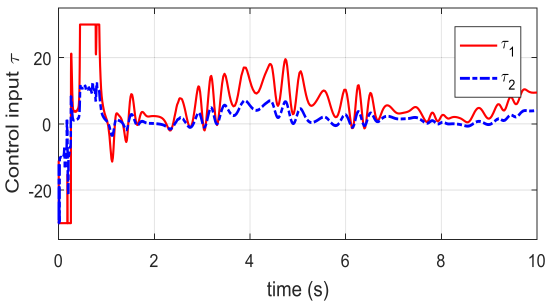

FIGURE 8. Control input τ under case 2.

V. CONCLUSION

Trajectory tracking control of EL system was studied in the presence of the actuator faults and system uncertainties. An adaptive compensation control scheme based on sliding mode control technique with auxiliary variable was developed such that the adverse influence caused by uncertain nonlinear term can be suppressed. The controller successfully accomplished tracking maneuver. And the stability of the tracking error was guaranteed by the Lyapunov theorem. Numerical simulations were included to support the theory analyses.

APPENDIX A

Proof of the three properties of Lemma 1:

① According to (3), one has

$$\frac{\partial\Gamma(\tau_i)}{\partial\tau_i} = \frac{e^{2c\tau_{iM}} - e^{-2c\tau_{iM}}}{\left(e^{c\tau_{iM}}e^{c\tau_i} + e^{-c\tau_{iM}}e^{-c\tau_i}\right)\left(e^{-c\tau_{iM}}e^{c\tau_i} + e^{c\tau_{iM}}e^{-c\tau_i}\right)} > 0 \tag{A.1}$$

From (4), we have $\Delta\tau_i = sat(\tau_i) - \Gamma(\tau_i)$, therefore $\Delta\tau_i$ satisfies

$$\begin{cases} 0 < \Delta\tau_i \le \tau_{iM} - \frac{1}{2c}\ln\left(\frac{e^{2c\tau_{iM}} + e^{-2c\tau_{iM}}}{2}\right), & if\ \tau_i \ge \tau_{iM}; \\ |\Delta\tau_i| \le \tau_{iM} - \frac{1}{2c}\ln\left(\frac{e^{2c\tau_{iM}} + e^{-2c\tau_{iM}}}{2}\right), & if\ |\tau_i| < \tau_{iM}; \\ -\tau_{iM} + \frac{1}{2c}\ln\left(\frac{e^{2c\tau_{iM}} + e^{-2c\tau_{iM}}}{2}\right) \le \Delta\tau_i \le 0, & if\ \tau_i \le -\tau_{iM}; \end{cases} \tag{A.2}$$

Based on (A.2), we obtain

$$|\Delta\tau_i| \le \tau_{iM} - \frac{1}{2c}\ln\left(\frac{e^{2c\tau_{iM}} + e^{-2c\tau_{iM}}}{2}\right) \tag{A.3}$$

Then, one can get $\lim_{c\to+\infty}\Delta\tau_i = 0$.

③ Since $\Gamma(\tau_i) = \frac{1}{2c}\ln\left(\frac{e^{c\tau_{iM}}e^{c\tau_i} + e^{-c\tau_{iM}}e^{-c\tau_i}}{e^{-c\tau_{iM}}e^{c\tau_i} + e^{c\tau_{iM}}e^{-c\tau_i}}\right)$, it has

$$\begin{cases} \lim_{\tau_i\to+\infty}\Gamma(\tau_i) = \lim_{\tau_i\to+\infty}\left[\frac{1}{2c}\cdot\ln\left(\frac{e^{2c\tau_{iM}} + e^{-2c\tau_i}}{1 + e^{c\tau_{iM}}e^{-2c\tau_i}}\right)\right] \\ \quad = \frac{2c\tau_{iM}}{2c} = \tau_{iM} \\ \lim_{\tau_i\to-\infty}\Gamma(\tau_i) = \lim_{\tau_i\to-\infty}\left[\frac{1}{2c}\cdot\ln\left(\frac{e^{2c\tau_i} + e^{-2c\tau_{iM}}}{1 + e^{-2c\tau_{iM}}e^{2c\tau_i}}\right)\right] \\ \quad = \frac{-2c\tau_{iM}}{2c} = -\tau_{iM} \end{cases} \tag{A.4}$$

Form (A.4), we can concluded that $|\Gamma(\tau_i)| \le \tau_{iM}$.

APPENDIX B

Proof of the three properties of Lemma 2: Obviously, we can obtain that

$$\begin{aligned} \|\bar{x}\| - \frac{\bar{x}^T\bar{x}}{\sqrt{\bar{x}^T\bar{x} + \zeta^2}} &= \frac{\|\bar{x}\|}{\sqrt{\bar{x}^T\bar{x} + \zeta^2}}\cdot\left(\sqrt{\bar{x}^T\bar{x} + \zeta^2} - \|\bar{x}\|\right) \\ &< \sqrt{\bar{x}^T\bar{x} + \zeta^2} - \|\bar{x}\| < \|\bar{x}\| + \zeta - \|\bar{x}\| < \zeta \end{aligned} \tag{B.1}$$

REFERENCES

[1] X. Y. Cai and M. de Queiroz, "Adaptive rigidity-based formation control for multirobotic vehicles with dynamics," *IEEE Trans. Control Syst. Technol.*, vol. 23, no. 1, pp. 389–396, Jan. 2015.
[2] J. R. Klotz, S. Obuz, Z. Kan, and W. E. Dixon, "Synchronization of uncertain Euler–Lagrange systems with uncertain time-varying communication delays," *IEEE Trans. Cybern.*, vol. 48, no. 2, pp. 807–817, Feb. 2018.
[3] H. Cai and J. Huang, "The leader-following consensus for multiple uncertain Euler-Lagrange systems with an adaptive distributed observer," *IEEE Trans. Autom. Control*, vol. 61, no. 10, pp. 3152–3157, Oct. 2016.
[4] K. Kumari, A. K. Behera, and B. Bandyopadhyay, "Event-triggered sliding mode-based tracking control for uncertain Euler–Lagrange systems," *IET Control Theory Appl.*, vol. 12, no. 9, pp. 1228–1235, 2018.
[5] G. Chen, Y. Yue, and Y. Song, "Finite-time cooperative-tracking control for networked Euler–Lagrange systems," *IET Control Theory Appl.*, vol. 7, no. 11, pp. 1487–1497, 2013.
[6] Q. K. Yang, H. Fang, J. Chen, Z.-P. Jiang, and M. Cao, "Distributed global output-feedback control for a class of Euler–Lagrange systems," *IEEE Trans. Autom. Control*, vol. 62, no. 9, pp. 4861–4885, Sep. 2017.
[7] F. A. Miranda-Villatoro, B. Brogliato, and F. Castaños, "Multivalued robust tracking control of Lagrange systems: Continuous and discrete-time algorithms," *IEEE Trans. Autom. Control*, vol. 62, no. 9, pp. 4436–4450, Sep. 2017.
[8] J. R. Klotz, Z. Kan, J. M. Shea, E. L. Pasiliao, and W. E. Dixon, "Asymptotic synchronization of a leader-follower network of uncertain Euler-Lagrange systems," *IEEE Trans. Control Netw. Syst.*, vol. 2, no. 2, pp. 174–182, Jun. 2015.
[9] S. Roy, I. N. Kar, J. Lee, and M. L. Jin, "Adaptive-robust time-delay control for a class of uncertain Euler–Lagrange systems," *IEEE Trans. Ind. Electron.*, vol. 64, no. 9, pp. 7109–7119, Sep. 2017.
[10] A. M. Bloch, N. E. Leonard, and J. E. Marsden, "Controlled Lagrangians and the stabilization of mechanical systems. I. The first matching theorem," *IEEE Trans. Autom. Control*, vol. 45, no. 12, pp. 2253–2270, Dec. 2000.
[11] H. Khalil, *Nonlinear Systems*, 3rd ed. Upper Saddle River, NJ, USA: Prentice-Hall, 2002.

[12] X. Wang, U. Kruger, G. W. Irwin, G. McCullough, and N. McDowell, "Nonlinear PCA with the local approach for diesel engine fault detection and diagnosis," *IEEE Trans. Control Syst. Technol.*, vol. 16, no. 1, pp. 122–129, Jan. 2008.
[13] Y. Zhang, N. Yang, and S. Li, "Fault isolation of nonlinear processes based on fault directions and features," *IEEE Trans. Control Syst. Technol.*, vol. 22, no. 4, pp. 1567–1572, Jul. 2014.
[14] M. Šimandl and I. Punčochář, "Active fault detection and control: Unified formulation and optimal design," *Automatica*, vol. 45, no. 9, pp. 2052–2059, 2009.
[15] A. E. Ashari, R. Nikoukhah, and S. L. Campbell, "Active robust fault detection in closed-loop systems: Quadratic optimization approach," *IEEE Trans. Autom. Control*, vol. 57, no. 10, pp. 2532–2544, Oct. 2012.
[16] B. Xiao and S. Yin, "Velocity-free fault-tolerant and uncertainty attenuation control for a class of nonlinear systems," *IEEE Trans. Ind. Electron.*, vol. 63, no. 7, pp. 4400–4411, Jul. 2016.
[17] Y. Song and J. Guo, "Neuro-adaptive fault-tolerant tracking control of Lagrange systems pursuing targets with unknown trajectory," *IEEE Trans. Ind. Electron.*, vol. 64, no. 5, pp. 3913–3920, May 2017.
[18] G. Chen, Y. Song, and F. L. Lewis, "Distributed fault-tolerant control of networked uncertain Euler–Lagrange systems under actuator faults," *IEEE Trans. Cybern.*, vol. 47, no. 7, pp. 1706–1718, Jul. 2017.
[19] Q. Hu, B. Xiao, and P. Shi, "Tracking control of uncertain Euler–Lagrange systems with finite-time convergence," *Int. J. Robust Nonlinear Control*, vol. 25, no. 17, pp. 3299–3315, 2015.
[20] J. Lyu, J. Qin, D. Gao, and Q. Liu, "Consensus for constrained multi-agent systems with input saturation," *Int. J. Robust Nonlinear Control*, vol. 26, no. 14, pp. 2977–2993, 2016.
[21] N. Fischer, Z. Kan, R. Kamalapurkar, and W. E. Dixon, "Saturated RISE feedback control for a class of second-order nonlinear systems," *IEEE Trans. Autom. Control*, vol. 59, no. 4, pp. 1094–1099, Apr. 2014.
[22] K. Shojaei and A. Chatraei, "A saturating extension of an output feedback controller for internally damped Euler–Lagrange systems," *Asian J. Control*, vol. 17, no. 6, pp. 2175–2187, 2015.
[23] D. H. Zhai and Y. Xia, "Adaptive control for teleoperation system with varying time delays and input saturation constraints," *IEEE Trans. Ind. Electron.*, vol. 63, no. 11, pp. 6921–6929, Nov. 2016.
[24] S. M. Smaeilzadeh and M. Golestani, "Finite-time fault-tolerant adaptive robust control for a class of uncertain non-linear systems with saturation constraints using integral backstepping approach," *IET Control Theory Appl.*, vol. 12, no. 15, pp. 2109–2117, 2018.
[25] A. Levant, "Robust exact differentiation via sliding mode technique," *Automatica*, vol. 34, no. 3, pp. 379–384, 1998.
[26] L. X. Wang, "Fuzzy systems are universal approximators," in *Proc. Int. Conf. Fuzzy Syst.*, San Diego, CA, USA, Mar. 1992, pp. 1163–1170.
[27] L. X. Wang and J. M. Mendel, "Fuzzy basis functions, universal approximation, and orthogonal least-squares learning," *IEEE Trans. Neural Netw.*, vol. 3, no. 5, pp. 807–814, Sep. 1992.

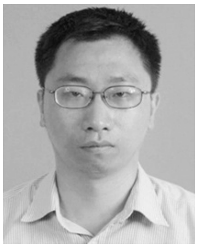

ZHANKUI SONG received the Ph.D. degree from the School of Control Science and Engineering, Dalian University of Technology, China, in 2014. He has been a Lecturer with the School of Information Science and Engineering, Dalian Polytechnic University, China. His research interests include robot motion control and adaptive nonlinear control.

KAIBIAO SUN received the Ph.D. degree from the School of Mathematical Sciences, Beijing Normal University, China, in 2008. He is currently an Associate Professor with the School of Control Science and Engineering, Dalian University of Technology, China. His research interest includes the modeling and identification of biological process.